Optik 125 (2014) 5241–5248

Contents lists available at ScienceDirect

Optik

journal homepage: www.elsevier.de/ijleo

Basic oxygen furnace steelmaking end-point prediction based on computer vision and general regression neural network

Hui Liu*, Bin Wang, Xin Xiong

Department of Automation, Kunming University of Science and Technology, Cheng Gong Campus, Kunming, Yunnan 650500, China

ARTICLE INFO

Article history:
Received 12 September 2013
Accepted 14 May 2014

Keywords:
BOF end-point
Image features
Prediction model
GRNN

ABSTRACT

End-point prediction is one of the most difficult problems in basic oxygen furnace (BOF) steelmaking process. To address this problem, some researchers have proposed some methods based on flame image processing and pattern classification. Because of the dynamically changing flame and real-time needs during the blowing process, there are still some issues that need to be solved. We propose a novel method based on accurate and fast multi flame features extraction and general regression neural network (GRNN). Firstly, flame images were acquired, and then the background of each image was removed via color similarity determination algorithm; secondly, color, texture, and boundary features were extracted; the fast and robust boundary and texture features were extracted by using the proposed methods, and these features were tested for their validity to the end-point prediction via comparing them with some other similar methods; finally, the prediction model was built using multi-features and GRNN. The experimental results demonstrated that it is accurate and fast to use the proposed method to the BOF end-point predict.

1. Introduction

The steel industry is an important raw material industry which supports the development of the national economy in China. The converter steel production reached 70% of the total production in the steel department. During the converter steelmaking process, the end-point control is a difficult problem. The accurate convert end-point control is significant to the production quality.

At present, the most common method in developing countries is to use the vice gun probing and experience judgment [1] method. The vice gun was immersed into the molten pool to detect the temperature and the carbon content, and the end-point was judged according to the detection result; the workers forecast the blowing data by watching the flame, then adjust the quantity of blowing oxygen and raw material in the converter. This approach relies on human experience and the worker's emotional state; therefore, it is ineffective to the end-point control. Some large steelmaking factories predict the end-point by using the photoelectric detection method to detect the changes of infrared laser via the furnace gas [2]; and some factories use the gas analysis method to test the chemical composition of the furnace gas [3–6]. These equipments are worked in the high temperature and corrosive environment for a long time, so the use and maintenance costs of the devices are very high; thus these methods cannot be used widely. In recent years, with the development of digital image processing and computer skill, some researchers proposed BOF end-point control methods based on flame image features extraction [7–11]. In [12], the gray level co-occurrence matrix (GLCM) was used to extract the BOF flame texture features, but the running time of this algorithm is too long due to the two times calculation. In [13], the BOF flame brightness and texture were extracted; the features, i.e., brightness, texture entropy, and texture angular second matrix features were found changed according to the BOF blowing stages. In [14], the researchers considered that the algorithms of flame image features extraction were complex and cannot meet the real-time requirements of the blowing process; they proposed a method of fusing infrared spectral radiant energy and image color feature to predict the end-point of the converter; as we know, in the steelmaking site, there are many high-temperature objects that radiate outward spectral energy, which affect the accuracy of the detection.

As to the methods of flame image features extraction, scholars have done a lot of research in this field. In [15], principal component analyses (PCA) were used to select the flame image multi-features, and this method was used in the online monitoring of the combustion system; but the conventional features extraction algorithms used in the method, i.e., boundary characteristics of circularity, high-temperature regional area, and flame color cannot meet the accurate and real-time needs in the online blowing application.

* Corresponding author. Tel.: +86 15368185621.
E-mail address: liuhui621@126.com (H. Liu).

http://dx.doi.org/10.1016/j.ijleo.2014.05.004
0030-4026/

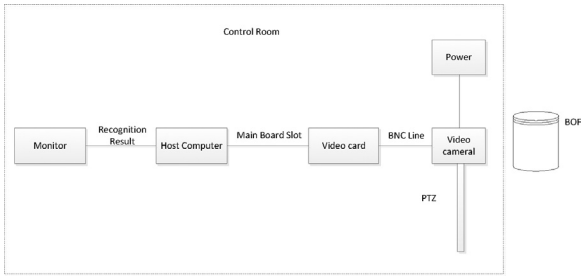

Fig. 1. Hardware connection of flame image acquisition system.

In [13], several features, including flame texture, color and so on were extracted to express the flame flicker characteristics, which can be used to separate the flame images from objects similar to the flame. In [16], the fractal dimension was used to describe the flame shape characteristic; this algorithm can be used to calculate the curvature of the boundary accurately, but it is time-consuming due to the need for many times of iterative calculation, and its weak robustness to the interference inflection point of the flame boundary.

In the converter blowing process, flame changes fast. Thus it is demanded that the image feature calculation algorithms should be rapid and accurate. This paper proposes novel methods in texture and boundary features extraction. For the texture feature, a gray level difference statistics method, which is special for random micro-texture, is proposed to extract the flame texture complexity. In order to describe the flame boundary bending complexity, a method of differential chain codes curvature calculation is proposed to calculate the boundary feature, which can eliminate the impact of small-scale corner. All the novel methods were compared with the classic methods in the aspect of accuracy and real-time to predict the end-point of converter.

2. Materials and methods

2.1. Data acquisition

Flame images, 640 × 480 size, were captured by a digital video camera in the steelworks of Kunming Iron & Steel Holding Co., Ltd.

The end-point prediction system is shown in Fig. 1. The flame image acquisition system is put into the control room; and the video camera shoots the flame images via the glass window. Images were processed and image features were extracted in the host computer, then the recognition result was printed on the monitor. We get blowing flame videos from the very beginning to the end, and the video flames were separated into two parts: one is the training set, and the other is the test set. The training set contains 41 flames that extracted each image every 30 s from the video; while the test set contains 100 flames that extracted each image every 12 s from the video.

2.2. Flame image segmentation

We use image segmentation techniques to remove the background area since our research only focuses on the flame. Because of the great color variation between the flame and the background, color similarity determination algorithm was used to remove the background.

Set m is a color vector, and on calculating the Euclidean distance between each pix of the image and m according to formula (1).

$$z = \begin{cases} Z_R = Z_G = Z_B = 0, & \text{if } D > T \\ z, & \text{if } D \le T \end{cases} \quad (1)$$

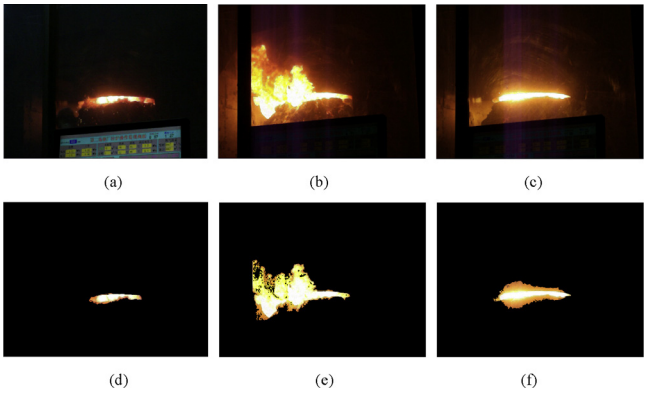

Fig. 2. The original and segmentation procedure for flame images. (For interpretation of the references to color in text, the reader is referred to the web version of the article.)

where D is the distance between m and pix; z is the new color pix vector value after the procedure; Z_R, Z_G, and Z_B stand for the R, G, and B color value, respectively. After the segmentation processing, the original and processed flame is shown in Fig. 2.

As shown in Fig. 2, (a)–(c) are the original flame images listed in the order of early, middle and later stage; (d)–(f) are the segmentation images of each stage. In the early stages of blowing, the color of the flame usually shows dark red and yellow, the texture is smooth, and the boundary curvature is not complex; in the middle stage of blowing, the flame color shows yellow and white, the texture is rough, and the boundary curvature is complex; in the end stage of blowing, the flame color shows white, the texture is smooth, and the boundary curvature is steady. All these flame characteristics reflect the impurity oxidation rate and the temperature in the furnace.

2.3. Features extraction

2.3.1. Color feature extraction

Color is one of the most important feature during the blowing process, because the flame color shows the different states of the blowing process. In the process of blowing, the color of the flame changes regularly.

Color moment is based on mathematical methods by calculating the moment to describe the color distribution. Color moments are usually calculated in the RGB space, and the color distribution is mainly concentrated in the lower order moments. Therefore, the first moment, the second moment, and the third moment are sufficient to express the color distribution of an image. They were defined as follows:

$$\mu_i = \frac{1}{N}\sum_{j=1}^{N} P_{ij} \quad (2)$$

$$\sigma_i = \left[\frac{1}{N}\sum_{j=1}^{N}(P_{ij} - \mu_i)^2\right]^{1/2} \quad (3)$$

$$\zeta_i = \left[\frac{1}{N}\sum_{j=1}^{N}(P_{ij} - \mu_i)^3\right]^{1/3} \quad (4)$$

where P_{ij} is the color value of number j pixel and number i color components; N is the total number of pixels of the image. The first moment of color shows the average intensity of each color component, the second and the third moment shows the variance and skewness of each color component, respectively.

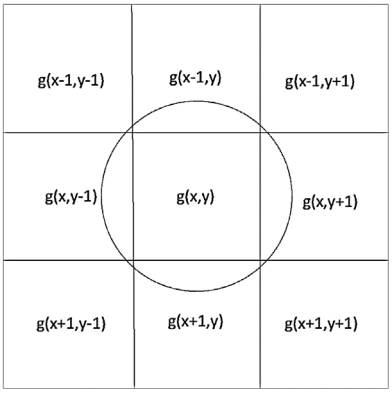

Fig. 3. Gray differential statistics.

2.3.2. Texture feature extraction

Flame image texture is formed by the different color transit. Its features reflect carbon content inside the furnace. In different states of burning, the roughness of the flame image shows differently. So the feature of texture roughness is very important to the end-point predict.

We used the proposed method to extract the texture features, which is texture gray scale difference static (GSDS). Before calculating the texture feature, the direction and scale of the GSDS should be defined according to the real needs, which called for the modeling of the difference static structure element. Set (x, y) is a pixel of an image, while $(x + \Delta x, y + \Delta y)$ is another one. The gray difference between the two pixels is $g_{\Delta}(x, y) = g(x, y) - g(x + \Delta x, y + \Delta y)$. $g_{\Delta}(x, y)$ is the gray difference. Because the flame texture belongs to random and micro texture structure type, the gray differences in all eight directions have statistical significance and the differential steps should be small. The gray differential direction and steps are shown in Fig. 3.

The gray differential of eight directions around pixel $g(x, y)$ should be calculated, then the differential statistical histogram of the whole image should be counted; the differential statistical texture expression of stochastic and micro-structure was defined as:

$$p(k) = \sum_{x=0}^{L-1}\sum_{y=0}^{L-1} C[k] = \sum_{x=0}^{L-1}\sum_{y=0}^{L-1}\left[\sum_{m=1}^{8} c(g(x, y) - g(x + \Delta x_m, -y + \Delta y_m))\right] \quad (5)$$

where $p(k)$ is the frequency of gray differential of the whole image; $c[k]$ is the frequency of gray differential within the structural element, its value is 0–255. m is the direction of the difference, its value is described in formula (6).

$$\begin{cases} \text{if } m = 1 \text{ then } \Delta x_m = 0, \quad \Delta y_m = 1 \\ \text{if } m = 2 \text{ then } \Delta x_m = -1, \quad \Delta y_m = 1 \\ \text{if } m = 3 \text{ then } \Delta x_m = -1, \quad \Delta y_m = 0 \\ \text{if } m = 4 \text{ then } \Delta x_m = -1, \quad \Delta y_m = -1 \\ \text{if } m = 5 \text{ then } \Delta x_m = 0, \quad \Delta y_m = -1 \\ \text{if } m = 6 \text{ then } \Delta x_m = 1, \quad \Delta y_m = 0 \\ \text{if } m = 7 \text{ then } \Delta x_m = 1, \quad \Delta y_m = 1 \end{cases} \quad (6)$$

Based on gray-scale difference histogram, the characteristic parameter should be calculated. Entropy (ENT) is a measure of randomness of an image. When the gray difference histogram is dispersed, the entropy is large, which means that the image has a greater degree of texture non-uniformity or complexity.

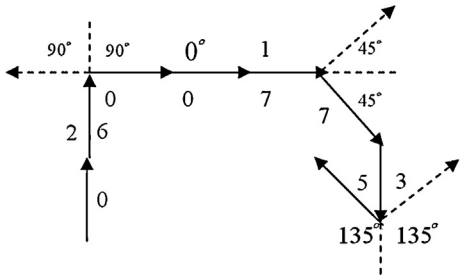

Fig. 4. Definition of the flame boundary difference chain code and curvature angle.

$$\mathrm{ENT} = -\sum_{i=0}^{255} p_{\Delta}(i) lg p_{\Delta}(i) \quad (7)$$

Thus, we choose the ENT to be the characteristic parameter to describe the texture feature of the image.

2.3.3. Boundary feature extraction

Flames boundary bending complexity reflects the intensity of combustion in the bath, the oxidation rate of the carbon or other elements, and the bath temperature. Thus, the complexity of the flame border has practical meaning. Burning flame boundary has some special particularity such as brief steady moment, and boundary line changes in multi-scale. Because the small-scale inflection point can cause errors in the calculation process, it should be eliminated.

Since the boundary curvature calculations can directly reflect the boundary complexity compared to other methods, a method based on boundary chain code curvature (BCCC) for calculating the flame boundary features is proposed in this paper.

The curvature is greater, which means the greater is the degree of the bending curve. The curvature is defined by the differential. Before calculating the differential curvature, the image should be preprocessed and should have got the flame boundary single connected region.

In Fig. 4, each arrow represents a sampling interval of boundary; the number beside the arrow stands for the differential chain code value. Angle value represents the two changing adjacent intervals. The dotted line represents an extension cord. There are four possible angle values existing in the flame boundary, and its value represents the changing direction at the inflection point.

We define K as the flame boundary curvature. In the single connected region, the average of a first-order differential chain code angle of all the boundary pixels is calculated in formula (8):

$$K = \frac{\sum_{i=1}^{N} \alpha_i}{N} \quad (8)$$

where N is the pixels number of the boundary line, θ is the value of the differential chain code, α is the differential chain code angle. First, we calculate the value of differential chain code of each pixel, and then calculate the value average of the entire pixel to be the curvature. The formula is defined in (9), according to the relationship between the chain code value and the differential chain code value.

$$\alpha = \begin{cases} 0 & \text{if } \theta = 0 \\ 180 - \left|\theta - 4\right| \times 45 & \text{if } \theta \neq 0 \end{cases} \quad (9)$$

Differential chain code curvature can be used to describe the boundary complexity characteristics. In order to verify the formula correctness, we use the triangle star, the five-pointed star, and the anise star for the test object as shown in Fig. 5.

Fig. 5. Algorithm verification of polygon.

According to formula (9), the chain code value of the three kinds of graphs is 18.3, 23.625, and 53.925, respectively. The calculation results match with the predicted results, indicating that the approach can describe the complexity of the boundary curvature effectively.

Before calculating the boundary feature, the fire boundary should be detected and processed fit to the curvature formula. The fire image boundary was detected and processed according to the following steps:

Step 1: Change the RGB segmentation image into gray, and extract the image boundary by using the morphology method.
Step 2: Boundary simply connected processing through calculating the boundary perimeter, and maintaining the longest one.
Step 3: Boundary polygon reconstruction. In order to smooth the boundary and reduce the calculation error, the border was fitted by a smooth polygon. The output graphic is shown in Fig. 6.

After getting the polygon boundary, then use the proposed method is used to calculate the boundary features.

2.4. GRNN recognition model

We use the generalized regression neural network to be the modeling method. The model can build the relationship between flame features and the blowing data, which are carbon content, phosphorus content, and the temperature. The BOF end-point can be judged according to the blowing data.

(a) (b)

Fig. 6. Reconstruction of flame boundary using polygonal approximation.

The forecasting modeling system need to design the number of input and output, and the network parameters.

In order to test the effect of different characteristic values, we designed four kinds of models, which are based on flame color features (M-C), texture features (M-T), boundary features (M-B), and multi-feature fusion (M-M). Each model makes the feature(s) as its input. The output of the model is the carbon content, phosphorus content, and the temperature in every prediction model.

As for the network parameters, there is only one parameter, named 'spread', that needs to be considered in GRNN. Spread is a threshold to control the sensitivity of the GRNN, and its value is usually obtained by a experimental method [17].

Converter blowing can be divided into three stages, named blowing early, mid and late. The aim of the predict model is to output the blowing data, and then to judge the state of that current image belongs to. According to some references and blowing experience, the blowing stage classification is based on the following rules as described by the MATLAB language.

```
if((c>=36&p>=16)|(c>=36&t<1540)|(p>=16&t<1540))
        flag=1;        % blowing early
elseif((c>=2.5&c<36&p>=7&p<16)|(c>=2.5&c<36&t<1640&t>=1540)|(p>=7&p<16&t<1640&t>
=1540))
        flag=2;        % blowing mid
else
        flag=3;        % blowing late
end
```

where c stands for the carbon content (%), p stands for the phosphorus content (%), t stands for the temperature (°C), and flag is the blowing stage; we use one, two and three for blowing early, mid and late, respectively.

3. Results and discussion

The features were obtained by the methods mentioned above. The predict models were built by using GRNN. In order to test the effectiveness of the feature methods, some others similar methods were compared.

In the test set image sequences, 1–20 are the early state of blowing, 21–80 are the mid state of blowing, and 81–100 are the late blowing state.

3.1. Color feature

The color flame image three-order moment feature (skewness) is shown in Fig. 7. Chart (a) is the color skewness feature of training set, and the image sequences are ordered by blowing early, mid and late. Chart (b) is the color skewness feature of the test set, then (c)–(e) is the output blowing data of the predict model based on GRNN. Chart (f) is the blowing state recognition result of color skewness feature based on the prediction model.

In order to compare the effectiveness between color skewness and color average value, which was frequently used, color mean feature was also extracted in the experiment. The recognition result is shown in Fig. 8.

There are some parameters used to evaluate the effect of recognition result; we chose three parameters to test the result, which are recognition rate, time consumed and the best spread value. The result is shown in Table 1.

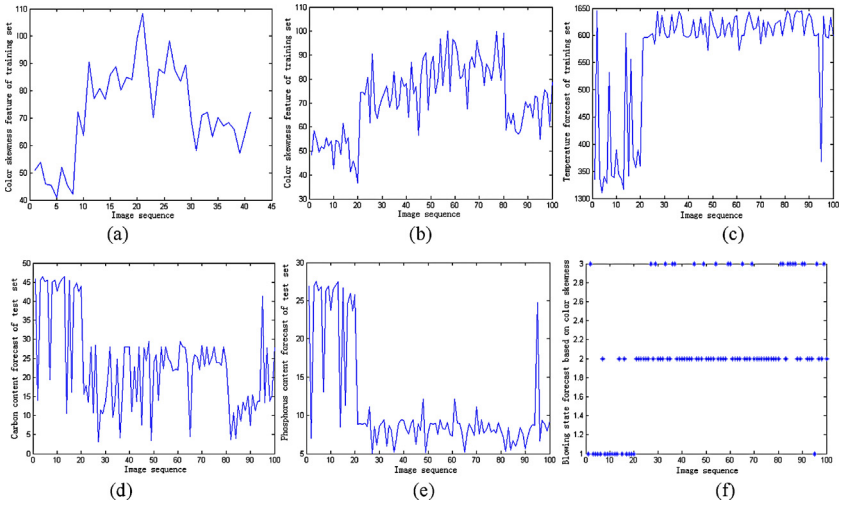

Fig. 7. Recognition results of three-order moment feature of flame image.

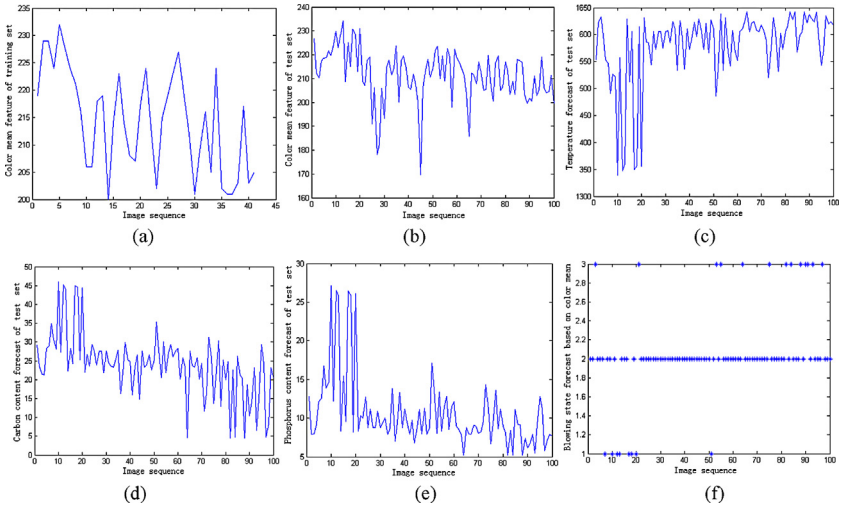

Fig. 8. Recognition results of flame image color mean feature.

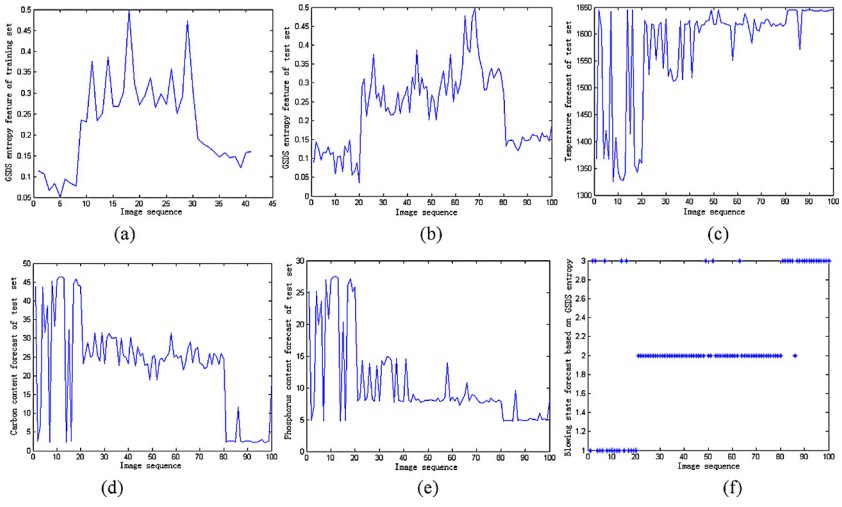

Fig. 9. Prediction output of gray differential statistics entropy feature.

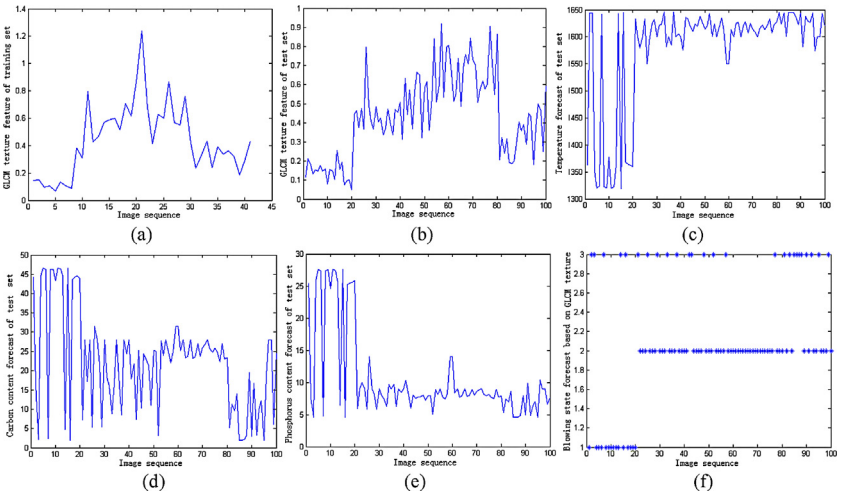

Fig. 10. Prediction output of Gary level co-occurrence matrix entropy feature.

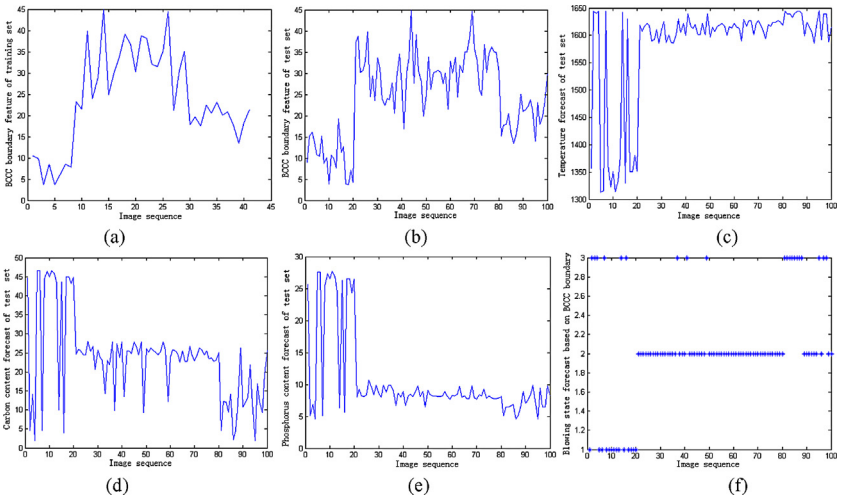

Fig. 11. Image recognition results of differential chain code boundary curvature feature.

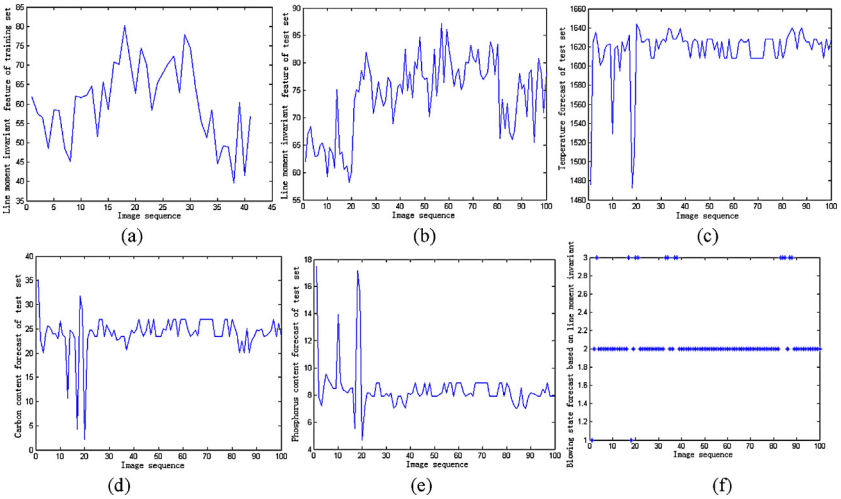

Fig. 12. Image recognition results of boundary line moment invariant feature.

Table 1
Contrast table of converter flame color feature extraction.

Color feature	Spread value	Recognition rate (%)	Time consumed (s)
Skewness	1.2	74	0.75
MEAN	1	67	0.35

Table 2
Recognition result data contrast of texture complexity feature.

Texture feature	Time consumed (s)	Spread value	Recognition rate (%)
GSDS	0.3254	0.005	91
GLCM	12.4427	0.01	74

Table 3
Boundary complexity feature recognition data comparison.

Boundary feature	Spread value	Time consumed (s)	Recognition rate (%)
BCCC	1	1.166	82
Line moment invariant	0.5	0.4334	61

3.2. Texture feature

We proposed a texture gray-scale difference static (GSDS) method. The recognition result is shown in Fig. 9. Chart (a) is the GSDS-based texture feature curve; (b) is the feature curve of test set. Charts (b)–(d) are the prediction results of blowing data.

In order to demonstrate the effectiveness of the proposed method, the recognition result was compared with the GLCM texture feature.

GLCM-based texture feature result is shown in Fig. 10.

The prediction result parameters of the three methods are shown in Table 2.

3.3. Boundary feature

The boundary feature proposed in this paper is called the BCCC method, the prediction result is shown in Fig. 11.

In order to compare with the proposed method, boundary line moment invariant-based feature extraction result is shown in Fig. 12.

The prediction parameters are shown in Table 3.

3.4. Multi-feature prediction model

All flame features including color, texture and boundary have contributions to the blowing data prediction. So in this experiment, the three kinds of flame features were fused together as the input of the GRNN model. The image processing and blowing data prediction flow chart is shown in Fig. 13.

The output curve of prediction model based on fusion image features and GRNN is shown in Fig. 14.

The recognition correction result is 89%, and time consumed for one image is 1.82 s.

4. Discussion

We analyze the output figures and tables, and compared them with the commonly used methods. The results are discussed as follows:

(1) When the prediction model is based on flame image color third moment feature, the model has a higher recognition rate and higher calculation speed than color mean feature. Because the color mean feature method needs to calculate the RGB components average value, the color mean feature does not include the relationship between the three components, which are very different in the blowing state. Unlike the color mean feature, the color third moment feature method takes into account the different components of RGB, not only reflecting the color average value, but also the variance and skewness values, so it has good recognition and prediction result. There are some substantial changes in the blowing data curve in Fig. 6, which is due to the rapid changes in the flame in mid and late state, and the maybe the image sequence is unstable at the moment.

(2) When the prediction model is based only on the texture feature, there are two methods used to extract the texture features. As shown in Figs. 8, 9 and Table 2, the method of gray differential statistics entropy feature has a higher recognition rate and higher calculation speed than the GLCM method. Because the GSDS method calculates the grayscale difference histogram, which can be construed as the one-dimensional function of gray value, the computational complexity is not high. The calculation scale and direction also were considered in the method, so it is suitable to calculate the small and natural kind of texture features. The biggest drawback of GLCM is its long time consumption, which is due to the two times calculation.

(3) When the prediction model is based on a boundary feature, the proposed method BCCC has a higher recognition rate but a lower calculation speed compared with the line moment invariant. Because the boundary chain code and bending complexity were calculated in BCCC, it can directly reflect the bending characteristics of the boundary. The other methods are commonly used to calculate the boundary feature indirectly. From the perspective of converter blowing, the texture calculation time of BCCC can be accepted.

(4) Based on the above three aspects of the analysis, image color third moment feature, gray differential statistics entropy feature are fused together as the input of the prediction model. The recognition rate and run-time meet the requirements of blowing data and state prediction.

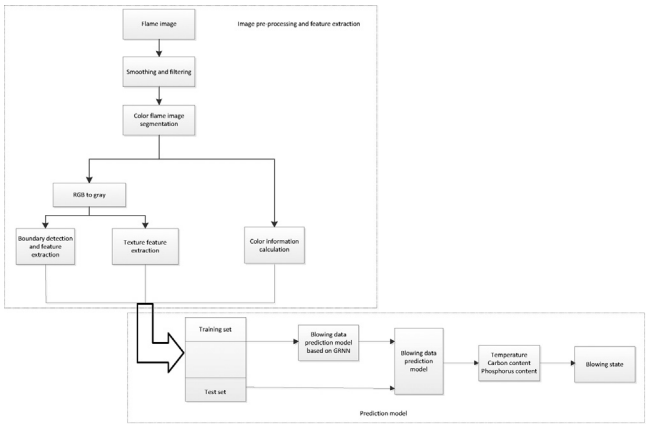

Fig. 13. Converter blowing data prediction based on multi-feature and GRNN.

5. Conclusions

BOF end-point prediction is a hard question during steelmaking. In order to find a rapid and low cost end-point control method, an end-point prediction method based on computer vision and GRNN is proposed in this work. The three kinds of vision features are studied. Considering the recognition rate and run-time needs, the method of gray differential statistics entropy texture feature and BCCC boundary features are also proposed. The compared experimental results show the effectiveness of the proposed methods. Finally, the three kinds of flame features are fused together, and the prediction model is built. The experimental result shows that

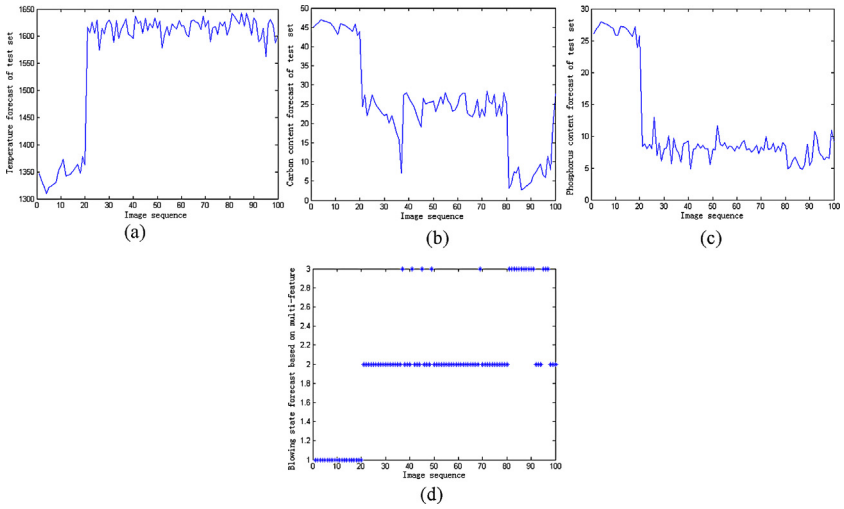

Fig. 14. Recognition results of GRNN using fusion image features.

the fusion prediction model can judge the blowing state quickly and effectively.

In the future study, the video dynamic features will be searched to improve the recognition rate.

Acknowledgements

We thank the workers in Kunming Iron & Steel Holding Co., Ltd. for their technical assistance. This work is supported by the National Natural Science Foundation of China (61263017), the Nature Science Foundation of Yunnan Province (2011FZ060), and the Nature Science Foundation of Kunming University of Science and Technology (KKSY201303120).

References

[1] H. Gruner, H.E. Wiemer, W. Fix, New metallurgical insight into BOF steelmaking and improved process control using sublance techniques and bottom gas stirring, Ironmak. Steelmak. 12 (3) (1985) 31–36.
[2] D. Merriman, Mass spectrometry for oxygen steel making control, Steel Times 25 (11) (1997) 439–440.
[3] K.Th. Mavrommatis, H.W. Gudenau, Use of on-line laser based analysis in steelmaking for improved monitoring and control of production, recycling and environmental processes, in: International Conference on Steel and Society/Steel Industry for Sustainable Society, Osaka, 2000, pp. 150–153.
[4] A.G. Coedo, I. Padilla, M.T. Dorado, Determination of minor elements in steelmaking flue dusts using laser ablation inductively coupled plasma mass spectrometry, Talanta 67 (1) (2005) 136–143.
[5] K. Takai, K. Iwasaki, Hyogo, System using electric furnace exhaust gas to preheat scrap for steelmaking, Environ. Int. 14 (2) (1988) 7.
[6] A.G. Coedo, T. Dorado, I. Padilla, Slurry sampling electrothermal vaporization inductively coupled plasma mass spectrometry for steelmaking flue dust analysis, Spectrochim. Acta B: At. Spectrosc. 55 (2) (2000) 185–196.
[7] L. Xu, W. Li, M. Zhang, S. Xu, J. Li, A model of basic oxygen furnace (BOF) endpoint prediction based on spectrum information of the furnace flame with support vector machine (SVM), Optik 122 (2011) 594–598.
[8] M. Hidenori, N. Akihiro, K. Fujio, Smoke detection in open areas with texture analysis and support vector machines, IEEE Trans. Electr. Electron. Eng. 7 (1) (2012) 59–70.
[9] J. Rong, D. Zhou, W. Yao, Fire flame detection based on GICA and target tracking, Opt. Laser Technol. 47 (1) (2013) 283–291.
[10] C. Lou, H. Zhou, Deduction of the two-dimensional distribution of temperature in a cross section of a boiler furnace from images of flame radiation, Combust. Flame 143 (1–2) (2005) 97–105.
[11] Q. Huang, F. Wang, J. Yan, Y. Chi, Simultaneous estimation of the 3-D soot temperature and volume fraction distributions in asymmetric flames using high-speed stereoscopic images, Appl. Opt. 51 (15) (2012) 2968–2978.
[12] J. You, S. Wang, X. Li, Y. Han, Estimate blowing final point by analysing texture features of top-blowing BOF vessel mouth flame, J. Univ. Sci. Technol. Beijing 22 (6) (2000) 524–528.
[13] D. Wang, X. Cui, E. Park, Adaptive flame detection using randomness testing and robust features, Fire Saf. J. 55 (1) (2013) 116–125.
[14] H.-Y. Wen, Q. Zhao, Y.-R. Chen, M.-C. Zhou, M. Zhang, L.-F. Xu, Converter endpoint prediction model using spectrum image analysis and improved neural network algorithm, Opt. Appl. 8 (4) (2008) 693–704.
[15] J. Chen, T. Hsu, C. Chien, Y. Cheng, Monitoring combustion systems using HMM probabilistic reasoning in dynamic flame image, Appl. Energy 87 (7) (2010) 2169–2179.
[16] F.C. Gouldin, An application of fractals to modeling premixed turbulent flames, Combust. Flame 8 (3) (1987) 249–266.
[17] P. Singh, M.C. Deo, Suitability of different neural networks in daily flow forecasting, Appl. Soft Comput. 7 (2007) 968–978.